

MEDICAL PHYSICS STUDENTS' TRAINING USING MCNP CODE

M A Al Kafi* and N Maalej

Department of Physics, King Fahd University of Petroleum and Minerals
Dhahran 31261, Saudi Arabia
malkafi@kfupm.edu.sa; maalej@kfupm.edu.sa

A A Naqvi

Center for Applied Physical Sciences, King Fahd University of Petroleum and Minerals
Dhahran 31261, Saudi Arabia
aanaqvi@kfupm.edu.sa

ABSTRACT

The Monte Carlo N-particle transport code MCNP 4B/4C was successfully used to train the students of Masters Degree Program in Medical Physics in King Fahd University of Petroleum and Minerals (KFUPM), Saudi Arabia. The code was used in class projects for two courses; Radiological Physics & Dosimetry and Radiation Therapy Physics. In Radiological Physics & Dosimetry, the code was used to calculate the x-ray dose distribution due to photon energies of 1, 2 and 5 MeV in geometries that mimic human chest, head and leg using aluminum for bone and water for soft tissue. The dose distributions for these energies were calculated at different depths of the geometries and compared with the calculated theoretical values. The simulated results show a very good agreement with the theoretical values obtained from the "Broad Beam Geometry". In Radiation Therapy Physics course, the code was used to simulate collimated linear accelerator photon beam interaction with a water phantom at 100cm source to surface distance (SSD). The percent depth dose (PDD) at different phantom depths for different photon beam energies (e.g., 1.25 MeV, 6 MeV) were calculated. The simulated results were in very good agreement with the published data. These studies show that MCNP is a very powerful tool in training medical physics students at KFUPM particularly in dosimetry and radiation transport calculations.

Key Words: Dosimetry, MCNP code, Broad beam geometry, simulation.

1 INTRODUCTION

Monte Carlo simulation is a stochastic technique that uses random numbers and probability statistics to obtain an answer. To physicists and medical scientists this simulation is one of the most important tools to study particle transport and interaction with matter as well as radiation protection and dosimetry. The nature of dose distribution in different parts of the body has a greater significance on radiation dosimetry. The percent depth dose inside different body depths has also very important implications in radiation therapy. We use the Monte Carlo n-particle transport code MCNP 4B/C in calculating dose distributions and percent depth dose in two class projects for Radiological Physics & Dosimetry and Radiotherapy Physics courses respectively to train Medical Physics students in KFUPM, Saudi Arabia.

* Corresponding Author

2 MATERIALS AND METHODS

2.1 MCNP Code:

Nowadays many Monte Carlo programs are available to meet different user needs. MCNP is a general purpose Monte Carlo n-particle transport code that is continuous-energy, generalized-geometry, time-dependent code and can be used for single or coupled neutron/photon/electron transport [1]. For neutrons, all reactions given in a particular cross-section evaluation are accounted for. For photons, the code takes account of incoherent and coherent scattering, the possibility of fluorescent emission or auger electrons after photoelectric absorption, absorption in pair production with local emission of annihilation radiation, and bremsstrahlung. A continuous slowing down model is used for electron transport that includes positrons, k x-rays, and bremsstrahlung but does not include external or self-induced fields. The neutron energy regime is from 10 MeV to 20 MeV, and the photon and electron energy regimes are from 1 keV to 1000 MeV. The code treats an arbitrary three-dimensional configuration of materials in geometric cells bounded by first- and second-degree surfaces and fourth-degree elliptical tori. The user creates an input file that is subsequently read by MCNP. This file contains information about the problems in areas such as [1]:

- The geometry specification
- The description of materials and selection of cross-section evaluations
- The location and characteristics of the neutron, photon, or electron source
- The type of answers or tallies desired
- Any variance reduction techniques used to improve efficiency

“Important standard features of MCNP include a powerful general source, criticality source, and surface source; both geometry and output tally plotters; rich collection of variance reduction techniques; a flexible tally structure; and an extensive collection of cross-section data [1]”.

2.2 Absorbed Dose:

Absorbed dose is a measure of the biologically significant effects produced by ionizing radiation. It can best be defined in terms of the related stochastic quantity, energy imparted ϵ (ICRU, 1980). The energy imparted by ionizing radiation to matter of mass m in a finite volume V is defined as:

$$\epsilon = (R_{in})_u - (R_{out})_u - (R_{in})_c - (R_{out})_c - \sum Q \quad (1)$$

where: $(R_{in})_u$ = radiant energy of uncharged radiation entering V

$(R_{out})_u$ = radiant energy of uncharged radiation leaving V

$(R_{in})_c$ = radiant energy of charged radiation entering V

$(R_{out})_c$ = radiant energy of charged radiation leaving V

$\sum Q$ = net energy derived from rest mass in V .

The absorbed dose D at any point P in V can be defined as:

$$D = \frac{d\epsilon}{dm} \quad (2)$$

where ϵ is the expectation value of the energy imparted in the finite volume V during some time interval, $d\epsilon$ is that for infinitesimal volume dv at point P , and dm is the mass in dv .

The old unit for dose is “rad”: $1 \text{ rad} = 100 \text{ ergs/g} = 10^{-2} \text{ J/kg}$

The SI unit for absorbed dose is the gray (Gy) and is defined as:

$$1 \text{ Gy} = 1 \text{ J/Kg}$$

In the presence of full charged particle equilibrium, the absorbed dose (D) to a medium can be calculated from the energy fluence ψ and the mass absorption coefficient $\frac{\mu_{en}}{\rho}$;

$$D = \psi \left(\frac{\mu_{en}}{\rho} \right) \quad (3)$$

2.3 Broad Beam Geometry:

Any attenuation geometry in which at least some non-primary rays reach the detector is called broad-beam geometry. “In ideal broad-beam geometry every scattered or secondary uncharged particle strikes the detector, but only if generated in the attenuator by a primary particle on its way to the detector, or by a secondary charged particle resulting from such a primary [2]”. For an ideal broad-beam geometry, the radiant energy of uncharged particles striking the detector through the attenuator at depth x is:

$$R_x = R_0 e^{-\mu_{en} x} \quad (4)$$

where R_0 is the primary radiant energy incident on the detector when the attenuator thickness $x=0$ and μ_{en} is the energy absorption coefficient. If n is the number of uncharged particles entering the attenuating medium, the energy fluence at any depth x of the attenuator is:

$$\psi = R_x n \quad (5)$$

Using equations (3), (4) and (5), for broad-beam geometry, the absorbed dose at any medium at a depth x can be obtained as:

$$D = \left(\frac{\mu_{en}}{\rho} \right) R_0 n e^{-\mu_{en} x} \quad (6)$$

If a source emits N photons isotropically, the energy fluence at a distance r from the source;

$$\psi = \frac{R_x N}{4\pi r^2} = \frac{R_0 N e^{-\mu_{en}x}}{4\pi r^2} \quad (7)$$

Then the absorbed dose can be written as:

$$D = \left(\frac{\mu_{en}}{\rho} \right) \frac{R_0 N e^{-\mu_{en}x}}{4\pi r^2} \quad (8)$$

For Radiological Physics & Dosimetry course, the Monte Carlo simulation code MCNP 4B/C was used to calculate the x-ray dose distribution in different geometries (fig. 1) that mimic human chest, head and leg.

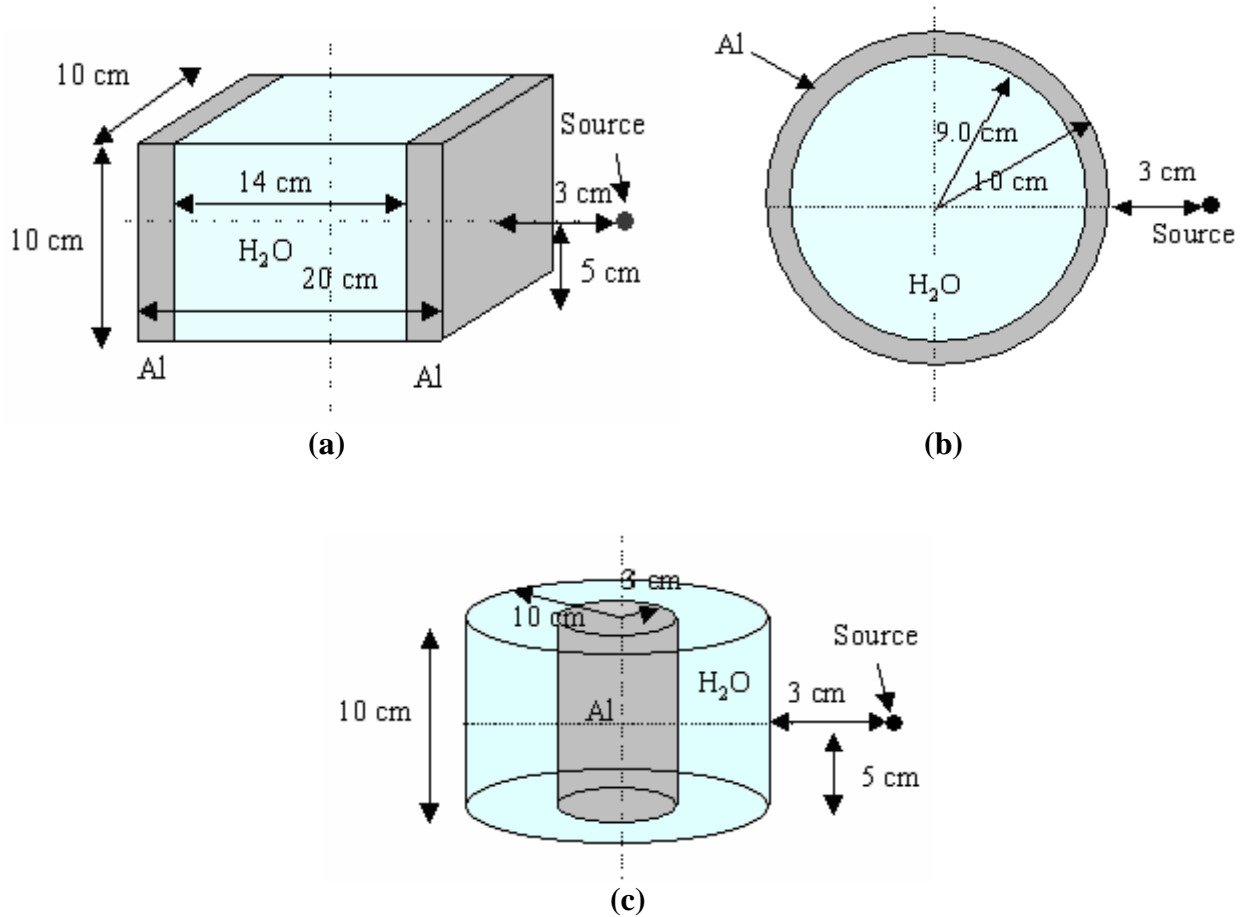


Figure 1. (a) Rectangular geometry mimicking human chest (b) Spherical geometry mimicking human head (c) Cylindrical geometry mimicking human leg

The chest was simulated by a rectangular geometry [fig. 1(a)]. The length along y-axis is 20cm and both the width and height are 10 cm. Both the outer left and right surfaces contain the material aluminum (equivalent to bone) of width 3cm. The inner part that has a length 14cm contains water (analogous to soft-tissue).

Figure-1 (b) shows a spherical geometry contains two concentric spheres that simulate human head. The inner sphere has a radius of 9cm and contains tissue equivalent water. Outside this is a spherical shell of radius 10cm contains aluminum simulating the skull. The gamma ray source is at 3cm from the outer surface of the geometry along y-axis.

Figure-1(c) shows a cylindrical geometry for leg where the inner cylinder contains aluminum (simulates the thigh bone) of radius 3cm. The outer part is a cylindrical shell of radius 10cm consisting of water (tissue equivalent). The height of the cylinder is taken 10cm on z-axis.

For each of the geometries, the source is placed at 3cm away from the surface of the geometry along y-axis. We calculate the dose distribution along y-axis due to the gamma ray source for 1, 2 and 5 MeV energies at the depths of 0.15, 0.5, 1.0, 1.5, 2, 3, 4, 5, 6, 7, 8, 10, 12, 14, 16 and 18cm from the surface. First MCNP 4C simulation code is used to calculate the dose distributions. 3×10^7 particles are used for the calculations. Theoretical calculations are done using broad beam geometry (eq. 8). The MCNP results are then compared with the theoretical results.

2.4 Percent Depth Dose (PDD):

Percent depth dose interrelates doses at points within a phantom. It is defined as the ratio, expressed as a percentage, of the absorbed dose at any depth d to the absorbed dose at a fixed reference depth d_{ref} , along the central axis of the beam, i.e.,

$$PDD = \frac{D_d}{D_{d_{ref}}} \times 100 \quad (9)$$

For orthovoltage and lower energy x-rays, the reference depth is usually taken at the surface ($d_{ref}=0$). For higher energies, the reference depth is taken at the position of the peak absorbed dose ($d_{ref}=d_m$). The parameters that affect the percent depth dose include the beam quality or energy, depth, field size and shape, source to surface distance (SSD) and beam collimation [3].

For Radiation Therapy Physics course, the MCNP code is used to simulate a linear accelerator problem to generate percent depth dose in a water equivalent cubic phantom (fig. 2). The size of the phantom is $30 \times 30 \times 30 \text{ cm}^3$. The photon source is a linear accelerator that is placed 100 cm away from the phantom surface (SSD=100cm) along z-axis. A lead (Pb) collimator of width 5 cm is placed on the path of the beam at 10 cm^2 from the source. The collimator opening is cut with a diverging angle such that it produces a $10 \times 10 \text{ cm}^2$ beam on the surface of the phantom. The size of the opening on the top of the collimator is $1 \times 1 \text{ cm}^2$ and at the bottom $1.5 \times 1.5 \text{ cm}^2$. We calculate the percent depth dose along the beam central axis inside the phantom due to the gamma rays for 1.25 MeV, and 6 MeV energies at the depths of 0.5, 1, 1.5, 2, 3, 4, 5, 6, 7, 8, 9, 10, 12, 14, 16, 18 and 20cm respectively from the surface of the phantom. The number of particles used here is 2.5×10^7 .

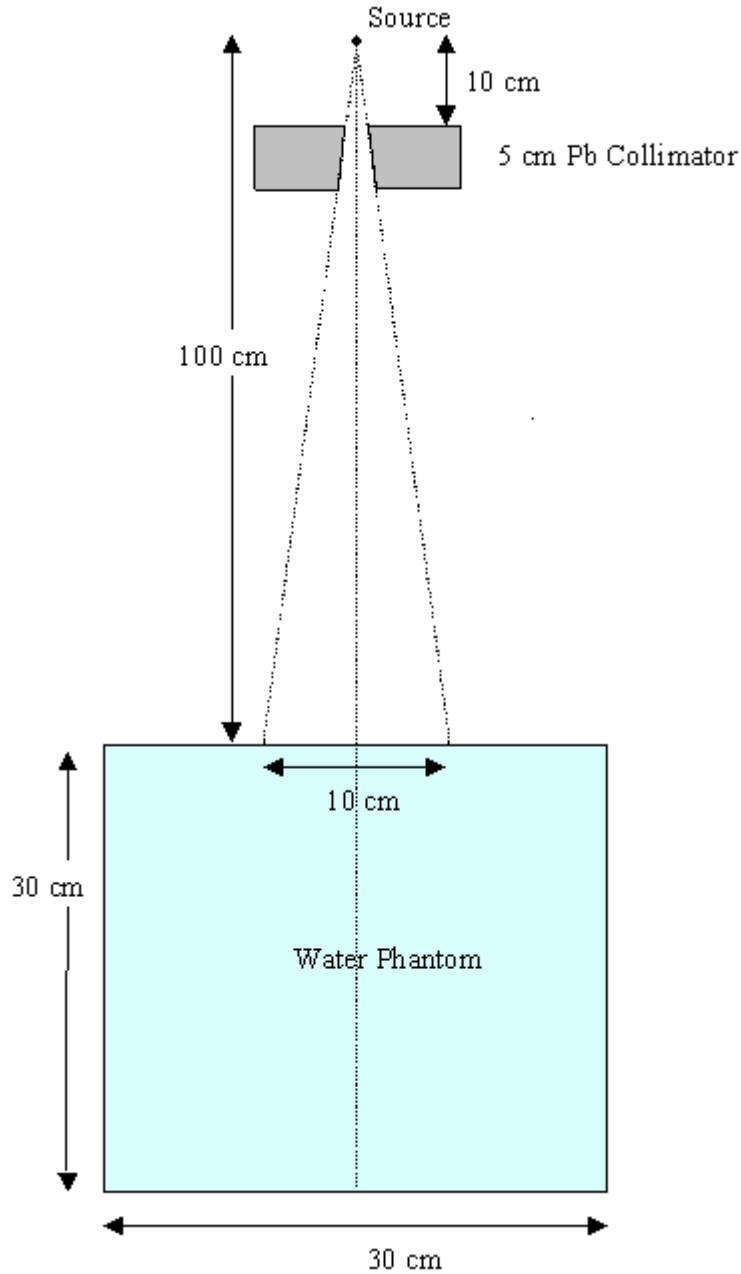


Figure 2. Geometry for measuring Percent Depth Dose

MCNP simulation code is used to calculate the dose distributions, from which the percent depth doses have been calculated for the given energies at the depths discussed above. Then the calculated data obtained from MCNP code are compared with the published data [4].

3 RESULTS AND DISCUSSION

The tables through I to III and figures 3-5 show the comparison between the theoretical dose distributions in different depths obtained from broad beam geometry and that obtained from the experimental MCNP simulation for different energies. For all the energies studied, the Monte Carlo simulation graphs fit quite well with Broad beam graph. Even it is almost impossible to differentiate between them at lower to middle depths. At Higher depths there are some variations which may be observed from the % differences in the tables. The cause of the variations is due to the statistical error in calculating the dose from the small number of particles reaching the detector at higher depths.

There are no significant but a little variations of the energy deposition observed in the boundaries of the materials because dose distributions near the interface of two materials depend on the associated energy and the atomic number of the materials. As observed by Detreix and Berbard (1986), a decrease in dose is observed just beyond the interface when photons go from a higher-Z to a lower-Z medium and an increase in the absorbed dose is seen beyond the interface when photons go from a lower-Z to a higher-Z medium.

Table I. Dose distributions in Chest geometry for Broad Beam geometry and MCNP Code

Depth (cm)	1 MeV			2 MeV			5 MeV		
	Dose (eV/gm) Broad Beam	Dose (eV/gm) MCNP Code	% Difference (±)	Dose (eV/gm) Broad Beam	Dose (eV/gm) MCNP Code	% Difference (±)	Dose (eV/gm) Broad Beam	Dose (eV/gm) MCNP Code	% Difference (±)
0.15	6.40E+09	6.53E+09	-1.95	1.08E+10	1.09E+10	-1.16	2.14E+10	2.19E+10	-2.60
0.5	5.06E+09	5.18E+09	-2.53	8.55E+09	8.66E+09	-1.30	1.70E+10	1.74E+10	-2.21
1	3.73E+09	3.85E+09	-3.07	6.35E+09	6.45E+09	-1.65	1.27E+10	1.29E+10	-1.72
1.5	2.85E+09	2.92E+09	-2.46	4.86E+09	4.92E+09	-1.06	9.82E+09	9.90E+09	-0.89
2	2.22E+09	2.29E+09	-3.22	3.82E+09	3.86E+09	-1.04	7.76E+09	7.84E+09	-0.98
2.85	1.53E+09	1.55E+09	-1.51	2.65E+09	2.69E+09	-1.56	5.44E+09	5.63E+09	-3.51
3.15	1.56E+09	1.60E+09	-2.11	2.72E+09	2.79E+09	-2.32	5.20E+09	5.37E+09	-3.28
4	1.17E+09	1.18E+09	-0.77	2.06E+09	2.08E+09	-1.36	3.95E+09	3.92E+09	0.77
5	8.72E+08	8.64E+08	0.92	1.53E+09	1.51E+09	1.82	2.97E+09	2.94E+09	1.05
6	6.68E+08	6.38E+08	4.49	1.18E+09	1.17E+09	1.33	2.30E+09	2.23E+09	3.05
7	5.25E+08	4.99E+08	4.96	9.32E+08	9.58E+08	-2.77	1.83E+09	1.77E+09	3.27
8	4.20E+08	4.28E+08	-1.86	7.51E+08	7.83E+08	-4.34	1.48E+09	1.42E+09	4.09
10	2.83E+08	2.76E+08	2.35	5.10E+08	5.24E+08	-2.70	1.02E+09	1.03E+09	-1.25
12	2.00E+08	1.77E+08	11.22	3.64E+08	3.62E+08	0.56	7.38E+08	6.87E+08	7.01
14	1.46E+08	1.36E+08	7.30	2.69E+08	2.51E+08	6.51	5.53E+08	4.84E+08	12.47
16	1.10E+08	8.68E+07	21.10	2.04E+08	1.75E+08	14.36	4.26E+08	3.74E+08	12.41
18	7.07E+07	5.96E+07	15.69	1.33E+08	1.29E+08	3.29	3.06E+08	2.46E+08	19.59

Table II. Dose distributions in Head geometry for Broad beam geometry and MCNP Code

Depth (cm)	1 MeV			2 MeV			5 MeV		
	Dose (eV/gm) Broad Beam	Dose (eV/gm) MCNP Code	% Difference (\pm)	Dose (eV/gm) Broad Beam	Dose (eV/gm) MCNP Code	% Difference (\pm)	Dose (eV/gm) Broad Beam	Dose (eV/gm) MCNP Code	% Difference (\pm)
0.15	6.40E+09	6.49E+09	-1.38	1.08E+10	1.09E+10	-0.98	2.14E+10	2.19E+10	-2.45
0.5	5.06E+09	5.13E+09	-1.45	8.55E+09	8.63E+09	-1.04	1.70E+10	1.74E+10	-1.98
0.85	4.07E+09	4.16E+09	-1.99	6.91E+09	6.97E+09	-0.88	1.38E+10	1.41E+10	-1.83
1.15	3.97E+09	4.01E+09	-1.14	6.76E+09	6.69E+09	0.97	1.26E+10	1.25E+10	0.48
1.5	3.34E+09	3.33E+09	0.21	5.69E+09	5.62E+09	1.25	1.06E+10	1.05E+10	1.17
2	2.66E+09	2.66E+09	0.00	4.55E+09	4.53E+09	0.41	8.53E+09	8.43E+09	1.19
3	1.79E+09	1.84E+09	-2.54	3.08E+09	3.11E+09	-1.05	5.81E+09	5.80E+09	0.09
4	1.28E+09	1.26E+09	0.94	2.21E+09	2.22E+09	-0.61	4.19E+09	4.08E+09	2.62
5	9.48E+08	9.64E+08	-1.72	1.65E+09	1.66E+09	-0.31	3.15E+09	3.10E+09	1.30
6	7.26E+08	7.41E+08	-2.09	1.27E+09	1.29E+09	-2.15	2.44E+09	2.37E+09	2.84
7	5.70E+08	5.66E+08	0.63	9.99E+08	1.02E+09	-2.40	1.94E+09	1.93E+09	0.48
8	4.57E+08	4.84E+08	-5.85	8.05E+08	8.22E+08	-2.08	1.57E+09	1.51E+09	3.56
10	3.07E+08	3.16E+08	-2.85	5.47E+08	5.58E+08	-1.96	1.08E+09	1.05E+09	3.06
12	2.17E+08	2.30E+08	-6.01	3.90E+08	3.90E+08	0.00	7.83E+08	7.32E+08	6.44
14	1.59E+08	1.53E+08	3.43	2.88E+08	2.83E+08	1.80	5.87E+08	5.35E+08	8.72
16	1.20E+08	1.13E+08	5.54	2.19E+08	1.98E+08	9.70	4.52E+08	4.12E+08	8.80
18	9.20E+07	9.48E+07	-2.97	1.70E+08	1.80E+08	-5.72	3.56E+08	3.08E+08	13.58

Table III. Dose distributions in Leg geometry for Broad beam geometry and MCNP Code

Depth (cm)	1 MeV			2 MeV			5 MeV		
	Dose (eV/gm) Broad Beam	Dose (eV/gm) MCNP Code	% Difference (\pm)	Dose (eV/gm) Broad Beam	Dose (eV/gm) MCNP Code	% Difference (\pm)	Dose (eV/gm) Broad Beam	Dose (eV/gm) MCNP Code	% Difference (\pm)
0.15	7.40E+09	7.42E+09	-0.28	1.25E+10	1.24E+10	0.22	2.29E+10	2.3E+10	-0.52
0.5	5.93E+09	5.94E+09	-0.19	1.00E+10	9.95E+09	0.51	1.84E+10	1.85E+10	-0.20
1	4.47E+09	4.45E+09	0.46	7.56E+09	7.48E+09	1.06	1.40E+10	1.39E+10	0.36
1.5	3.48E+09	3.44E+09	0.98	5.90E+09	5.80E+09	1.59	1.09E+10	1.08E+10	1.24
2	2.77E+09	2.75E+09	0.99	4.71E+09	4.66E+09	1.15	8.78E+09	8.64E+09	1.58
3	1.87E+09	1.91E+09	-2.51	3.19E+09	3.21E+09	-0.49	5.98E+09	5.95E+09	0.52
4	1.33E+09	1.34E+09	-0.56	2.28E+09	2.28E+09	0.00	4.31E+09	4.2E+09	2.49
5	9.88E+08	9.83E+08	0.48	1.70E+09	1.69E+09	0.35	3.24E+09	3.12E+09	3.53
6	7.57E+08	7.73E+08	-2.12	1.31E+09	1.31E+09	0.00	2.51E+09	2.42E+09	3.45
6.85	6.15E+08	6.19E+08	-0.54	1.07E+09	1.05E+09	1.56	2.06E+09	2.01E+09	2.44
7.15	4.97E+08	5.18E+08	-4.23	8.65E+08	8.68E+08	-0.31	1.80E+09	2.01E+09	-11.65
8	3.98E+08	4.17E+08	-4.95	7.00E+08	6.95E+08	0.68	1.47E+09	1.4E+09	4.86
10	2.46E+08	2.43E+08	1.51	4.44E+08	4.4E+08	0.72	9.57E+08	9.5E+08	0.72
11	1.98E+08	1.84E+08	6.73	3.60E+08	3.56E+08	1.12	7.87E+08	7.6E+08	3.38
12	1.60E+08	1.61E+08	-0.70	2.95E+08	2.97E+08	-0.60	6.53E+08	6.22E+08	4.69
14	1.29E+08	1.06E+08	17.90	2.42E+08	1.85E+08	23.64	5.07E+08	4.35E+08	14.22
16	9.72E+07	7.39E+07	23.93	1.84E+08	1.64E+08	10.73	3.91E+08	3.04E+08	22.29
18	7.48E+07	6.48E+07	13.36	1.43E+08	1.17E+08	17.99	3.08E+08	2.66E+08	13.59

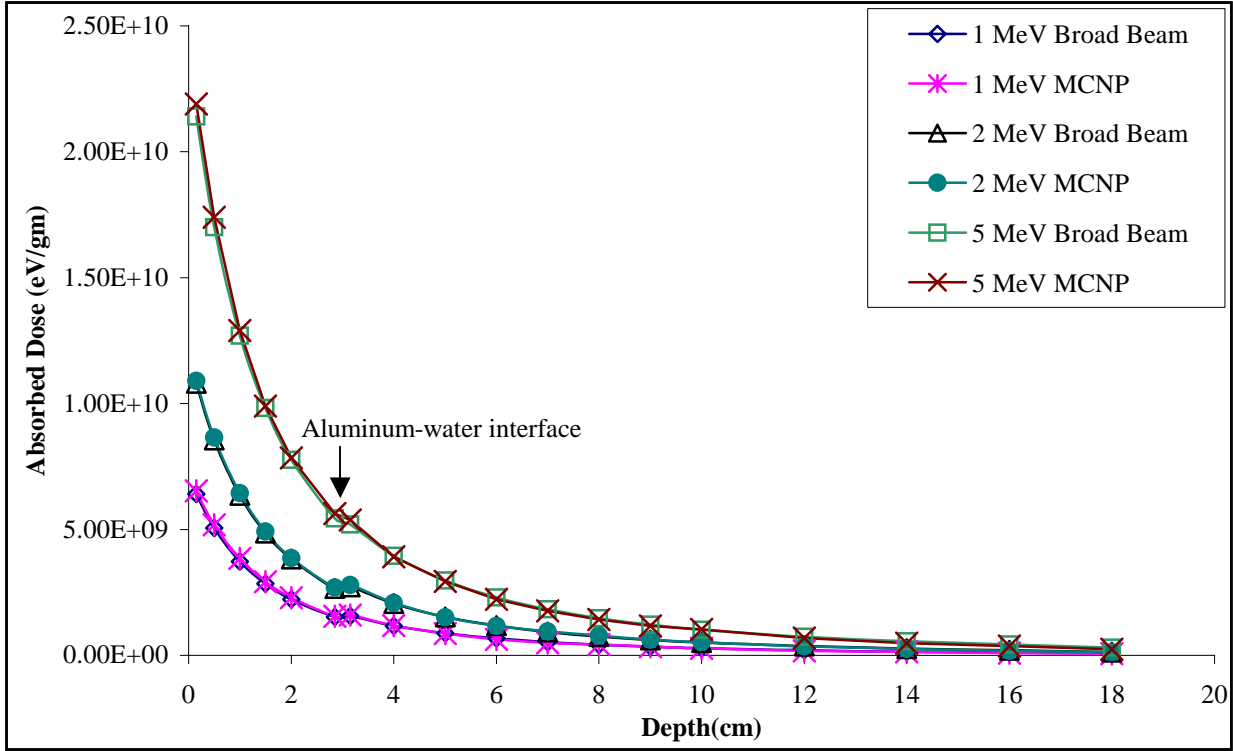


Figure 3. The absorbed dose as a function of depth in the chest simulated geometry.

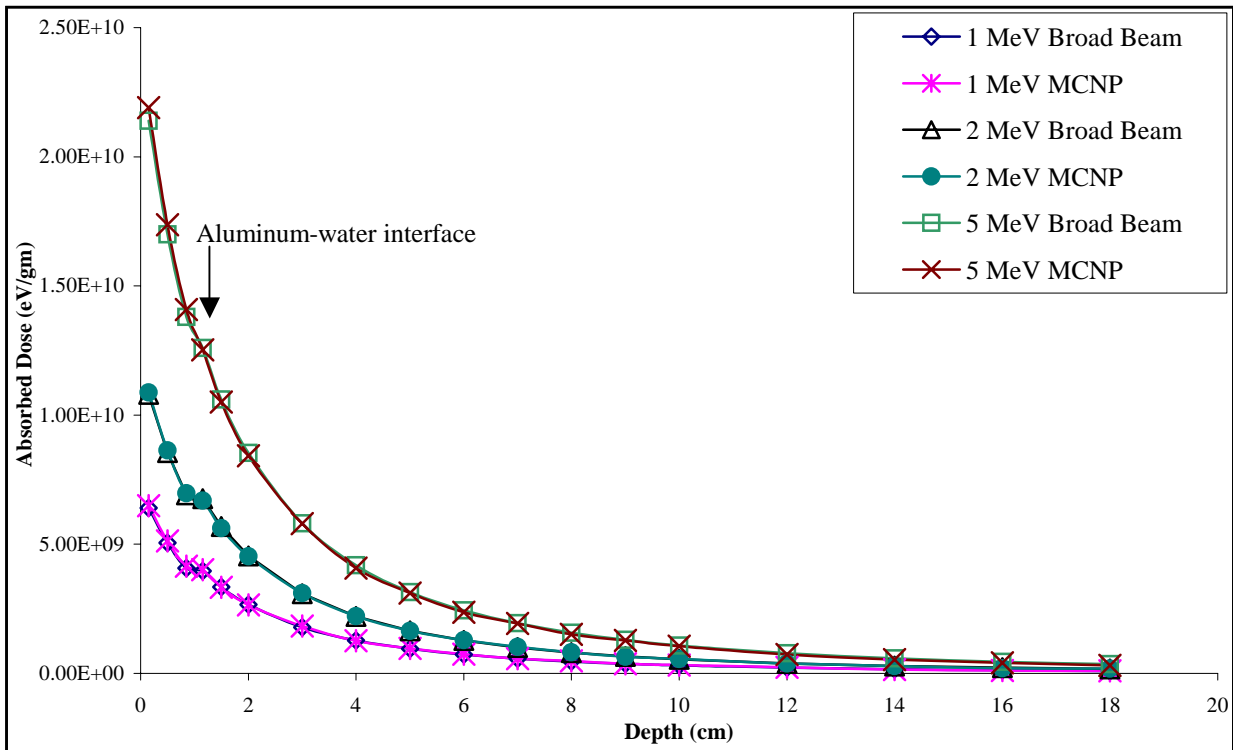


Figure 4. The absorbed dose as a function of depth in the head simulated geometry.

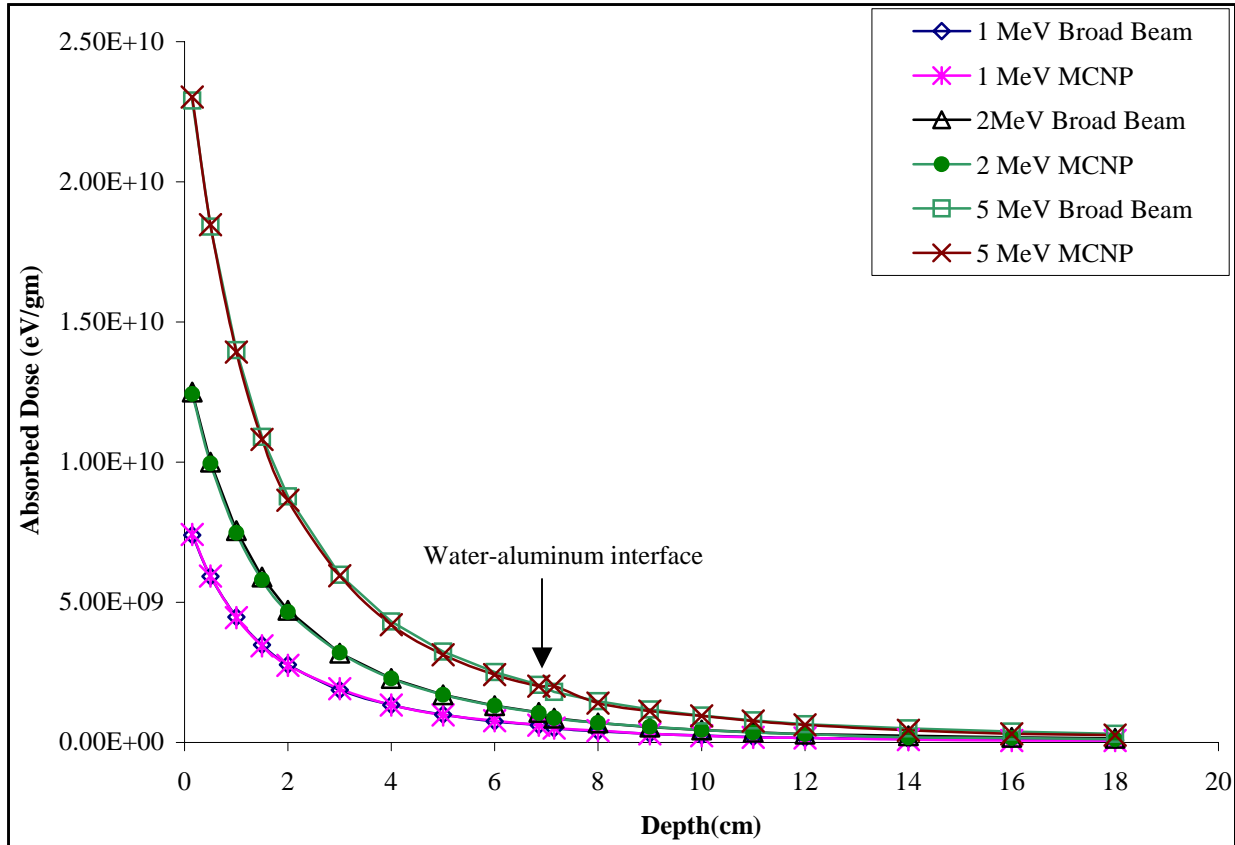


Figure 5. The absorbed dose as a function of depth in the leg simulated geometry.

The dose distribution along with the percent depth dose with respect to the maximum dose at d_{max} for 1.25 MeV and 6MeV photons at different depths in the water phantom is tabulated in the table IV. The experimental depth dose distribution is calculated from the data obtained from the results of Monte Carlo MCNP 4C code using eq. 9. The maximum dose occurs at $d_{max} = 0.15$ cm and 1.5 cm respectively for 1.25 MeV and 6 MeV beams whereas the actual values are 0.5cm and 1.5 cm respectively. The published data for percent depth dose are also given in the table. Figures 6 and 7 show the comparison between them. The fitted curves are made by drawing through the average points to overcome the fluctuations of data points. For both the energies studied the MCNP results shows a good similarity between the published data curve and fitted experimental curve. Columns 5 and 9 of the table represent the percentage difference between experimental MCNP results and published data. For higher depths the difference is more pronounced for both the energies which is due to the statistical error of counting less number of particles reaching the detector.

Table IV. Percent Depth Dose data for MCNP and Published data for different energies

Depth (cm)	1.25 MeV				6 MeV			
	Dose (eV/gm/particle) MCNP code	Percent Depth Dose (MCNP Code)	Percent Depth Dose (Published data)	% Difference (±)	Dose (eV/gm) MCNP code	Percent Depth Dose (MCNP Code)	Percent Depth Dose (Published data)	% Difference (±)
0.15	3.13E-07	100.00	98.0	-2.04	8.95E-07	98.41	58.5	-68.22
0.5	3.04E-07	97.36	100.0	2.64	9.00E-07	98.91	86.5	-14.35
1	2.99E-07	95.56	98.6	3.08	9.00E-07	98.96	99.0	0.04
1.5	2.99E-07	95.56	96.25	0.72	9.10E-07	100.00	100.0	0.00
2	2.98E-07	95.38	93.9	-1.57	8.77E-07	96.39	99.0	2.64
3	2.87E-07	91.72	89.3	-2.71	8.68E-07	95.41	95.0	-0.43
4	2.87E-07	91.75	84.7	-8.32	8.20E-07	90.18	91.0	0.90
5	2.56E-07	82.02	80.1	-2.39	7.74E-07	85.14	86.0	1.00
6	2.54E-07	81.25	75.5	-7.62	7.36E-07	80.92	82.5	1.92
8	2.25E-07	72.01	70.9	-1.57	6.93E-07	76.18	78.5	2.95
10	2.07E-07	66.19	66.4	0.31	7.01E-07	77.11	74.5	-3.50
11	1.88E-07	60.04	57.8	-3.88	6.02E-07	66.16	67.0	1.26
12	1.63E-07	52.20	50.3	-3.78	6.18E-07	67.97	60.0	-13.28
14	1.53E-07	48.85	43.9	-11.27	5.46E-07	60.02	54.0	-11.14
16	1.35E-07	43.24	38.3	-12.90	4.71E-07	51.74	48.5	-6.67
18	1.37E-07	43.96	33.5	-31.22	4.82E-07	53.00	43.5	-21.83
20	9.14E-08	29.23	29.3	0.25	4.67E-07	51.37	39.0	-31.72

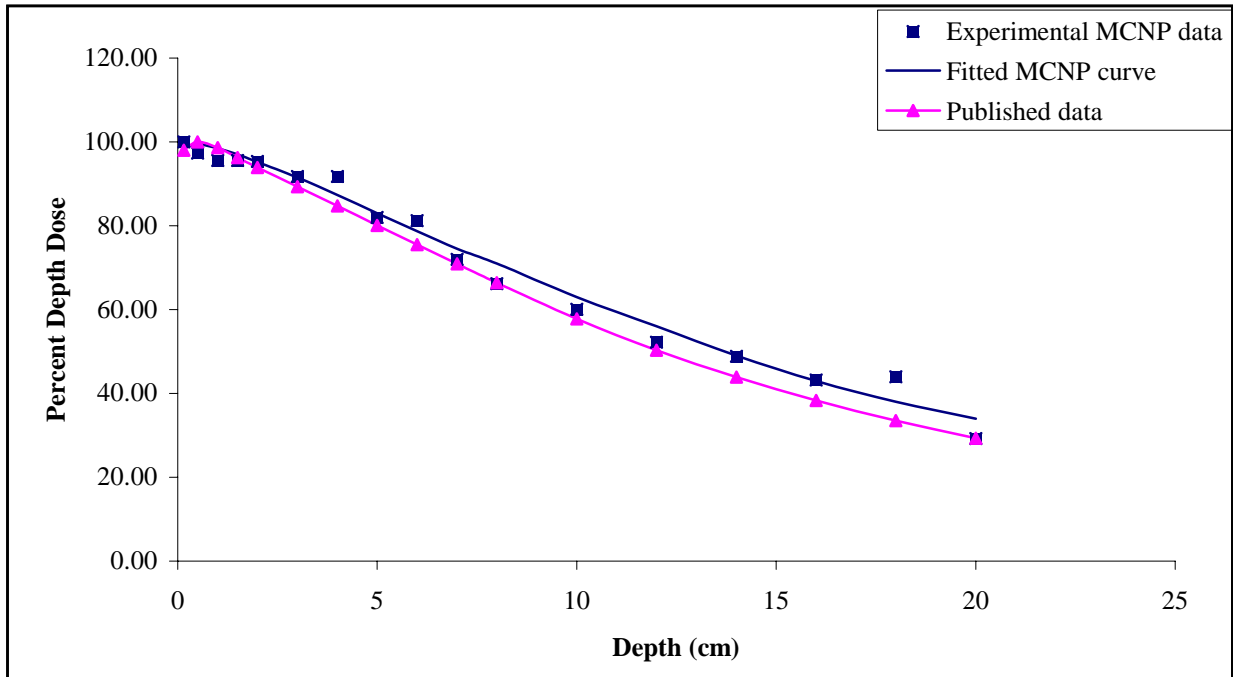


Figure 6. Percent Depth Dose (PDD) as a function of depth in water for 1.25 MeV beam.

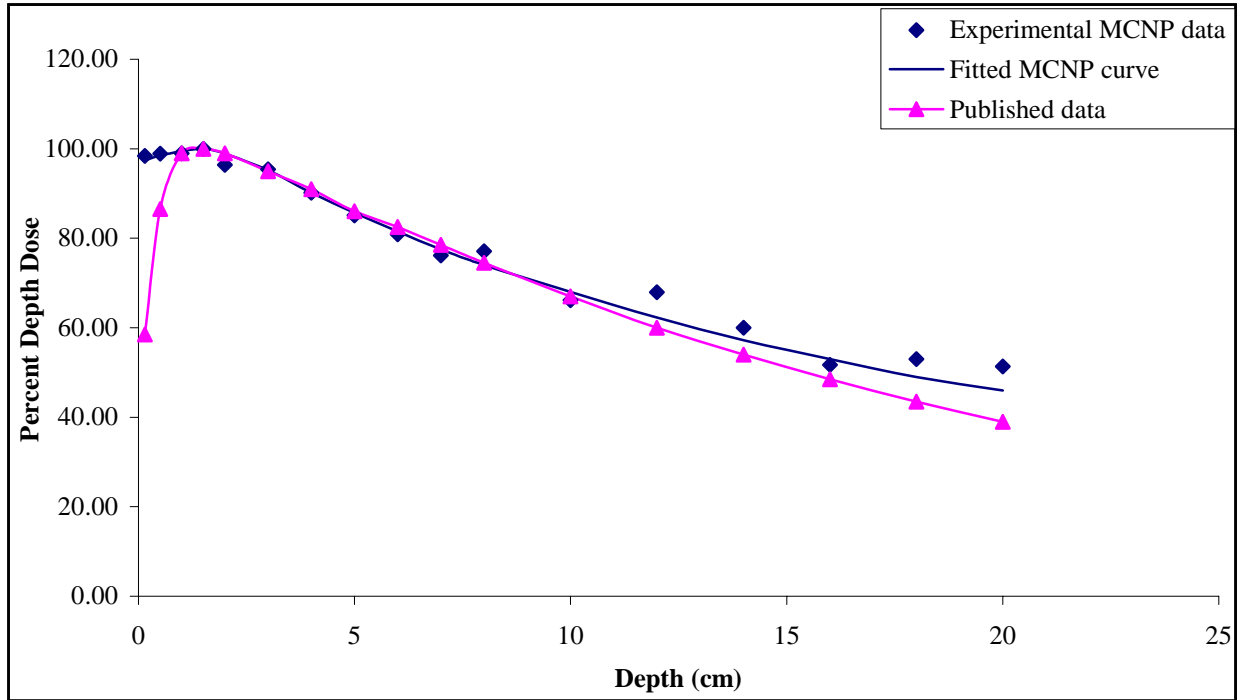


Figure 7. Percent Depth Dose (PDD) as a function of depth in water for 6 MeV beam.

4 CONCLUSIONS

Monte Carlo simulation code MCNP in the present projects give a good approximation of the theory and published data. However, in theoretical calculations of dose distribution, the effects due to the irregular shape of the geometries were not taken into account whereas MCNP includes those effects. For percent depth dose, the actual clinical conditions like temperature, pressure, humidity, etc., were not considered for MCNP calculations. In spite of the above-mentioned limiting factors, MCNP results agree well with the theoretical and published data. So MCNP can be a very useful method to simulate real problems where clinical techniques are not possible. In the Physics department of King Fahd University of Petroleum and Minerals, the code serves as a very powerful tool to train Medical Physics students especially in Radiation Therapy and Dosimetry calculations.

5 REFERENCES

1. Judith F. Briesmeister, Editor, *MCNP-A general Monte Carlo N-particle Transport Code (Version 4B)*, Los Alamos National Laboratory Manual, LA-12625-M (1997).
2. Frank H. Attix, *Introduction to Radiological Physics and Radiation Dosimetry*, John Wiley & Sons, Inc. New York, USA (1986).
3. Faiz M. Khan, *The Physics of Radiation Therapy*, Lippincott Williams & Wilkins, USA (1985)
4. H. E. Johns and J. R. Cunningham, *The Physics of Radiology*, 4th ed., Charls C Thomas, Springfield, IL, USA (1983)